Jordan Journal of Civil Engineering, Volume **12**, No. **3**, **2018**

Investigation on Interaction Curves of FRP-Reinforced Concrete Columns

Jamshid Esmaeili [1)]***, Masoud Farzam*** [2)] ***and Hadi Hamedi Baranlou*** [3)]

[1)] Professor, The University of Tabriz, Iran. E-Mail: J-esmaeili@tabrizu.ac.ir
[2)] Professor, The University of Tabriz, Iran. E-Mail: mafarzam@tabrizu.ac.ir
[3)] Engineer, The University of Tabriz, Iran. E-Mail: h-hamedibaranloo91@ms.tabrizu.ac.ir

ABSTRACT

Reinforcement of buildings and evolution of design codes are necessary due to the failure of buildings during earthquakes of any scale. Due to the seismicity of Iran and the tendency toward the use of concrete buildings, columns' resistance against earthquake forces can play an important role in the reinforcement of an entire structure. One of the most common ways of reinforcing concrete columns to upgrade and retrofit their structural function is the use of FRPs (fiber-reinforced polymers). Moreover, studies have shown that concrete columns reinforced with FRP retrofit would increase the flexural strength of columns, since almost all concrete columns with axial loads and bending moment are affected. In this research, by using ANSYS 15.0, concrete columns were modeled once without FRPs and then by wrapping one, two, three and four FRP-layers. The size of columns is doubled for studying the effect of the increased size of columns on the interaction diagrams. These columns were analyzed by exerting eccentric axial loads and the interaction diagrams were obtained in different states. The results of the analysis showed that increasing the number of layers somewhat increases the strength. However, the excess of layers is not cost-effective.

KEYWORDS: Reinforced concrete columns, Interaction curves, ANSYS finite element software, FRPs.

INTRODUCTION

For the reinforcement of concrete buildings, various solutions, such as adding harness straps, reinforced concrete shear walls, perimeter frames and the use of FRP, have been suggested. The use of FRP, because of its specific and unique features, has been considered in recent years.

Extensive research on retrofitting reinforced concrete columns has been conducted in the past three decades, which indicated that the FRP increases the load-bearing capacity of the column. The lifetime of many of reinforced concrete structures in Iran and other parts of the world is more than a decade and these structures have been damaged because of natural disasters, such as earthquakes, wind, material fatigue or corrosive agents. Since these structures are important and there are plenty of them, their replacement with new structures often lacks economic justification and is impractical. However, the reinforcement of the above-mentioned structures in most cases is necessary, economical and affordable.

Several studies have been conducted on the confinement of concrete in FRP. Several studies have examined the factors and parameters that influence the behavior of the encapsulated samples. Mirmiran et al. (1998) studied the effects of section shape, length to diameter ratio and adhesion between concrete and the FRP coating on the effectiveness of their confinement

Received on 20/1/2018.
Accepted for Publication on 14/4/2018.

and concluded that the effect of confinement on square columns is less than on circular ones. Also, the impact of the ratio of length to diameter on strength and ductility is small.

Parvin and Wang (2001) modeled columns confined in FRP with eccentric load by using finite and limited element MARC software. Mostofinezhad and Saadatmand (2008) presented equations for determining pressure resistance and ultimate axial strain of FRP-confined concrete and modeled the behavior of FRP-confined concrete under axial load and bending moment (anchor) using ANSYS. The model proposed by these researchers considers the effect of biaxial tensile and compressive stresses on the rupture strain of FRP. They also examined columns with confinement along their entire height or just at the plastic zone near the connection. Afterwards, they compared the buckling load of reinforced concrete columns (with the column entire height confined) to the buckling load of non-confined columns.

FINITE ELEMENT MODELING

The software used in the present numerical parametric study was ANSYS 15.0 SOLID65, which was used in order to model the concrete sections of the volume element. This element has eight nodes and each node has three degrees of transition freedom. This element was used in authentic parametric studies, like those conducted by Hadi (2007) and Mostofinezhad and Saadatmand (2008), who used similar conjunctions and connectors for which detailed results were presented. The linear elements of LINK 8 and SHELL 181 have been used for bars and FRP modeling, respectively. These elements were from Help ANSYS and related articles.

THE YIELDING CRITERION (MEASURE) FOR THE MATERIALS

The von Mises yielding measure was used to consider the plastic behaviors of steel and concrete under combined stress. For modeling the stirrup reinforcement bars, steel with a yielding stress of 363 MPa and ultimate stress of 571 MPa was used and for modeling the longitudinal reinforcement bars, steel with a yielding stress of 538 MPa and ultimate stress of 677 MPa was used. The stress-strain values of concrete are presented in Figure 1.

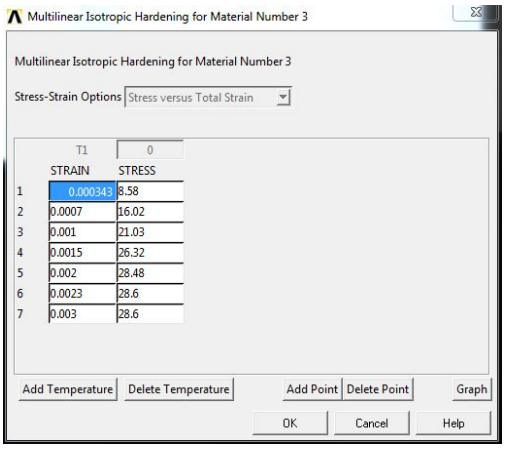

Figure (1): Stress-strain values of concrete

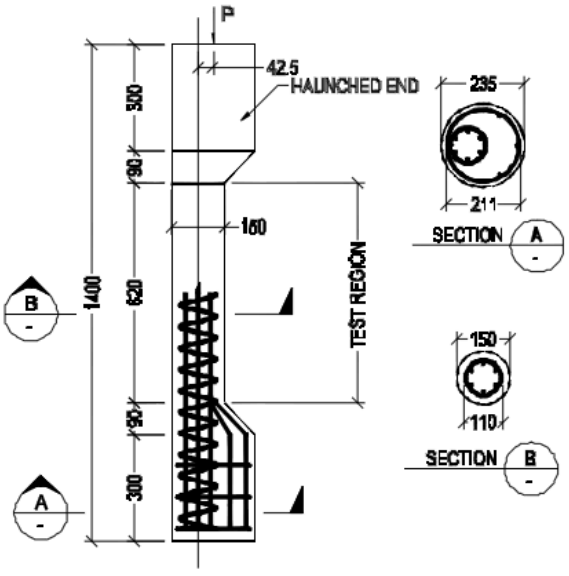

Figure (2): Characteristics of analytical samples

METHODOLOGY

All analytical samples were obtained from the experiments conducted by Hadi (2007). The characteristics of analytical samples are shown in Figure 2.

RESEARCH PROCEDURE

First, non-coated FRP circular concrete column was modeled and analyzed in ANSYS. Afterwards, the column was reinforced and analyzed with one, two, three and four FRP coatings.

Next, the size of the section was doubled to investigate the effect of increasing the size of the column on the axial load-bending moment interaction curve of the column and the analysis results were compared.

RESULTS AND DISCUSSION

The results derived from ANSYS for the M series samples are presented in Table 1.

Table 1. Distribution of net axial load, balance point of the section and net flexural column in the M series samples

	M0		M1		M2		M3		M4	
	Pn(N)	Mn(N.mm)	Pn(N)	Mn(N.mm)	Pn(N)	Mn(N.mm)	Pn(N)	Mn(N.mm)	Pn(N)	Mn (N.mm)
Net axial load	388723	0	480498	0	604883	0	724890	0	810921	0
Balance point of the section	277651	6211053	127995	27228376	233453	47699117	267842	49952533	380539	65787582
Net flexural column	0	964200	0	20122643	0	41625730	0	50554176	0	71470815

Figures 3 and 4 depict the distribution of stress under net axial load and net bending moment conditions in the absence of FRP (M0). Figures 5 and 6 show the distribution of stress in the net axial load and bending moment states with a layer of FRP (M1). Figures 7 and 8 show the distribution of stress in the net axial load and net bending moment states with two layers of FRP (M2). Figures 9 and 10 show the distribution of stress in the net axial load and net bending moment states with three layers of FRP (M3). Figures 11 and 12 illustrate the distribution of stress in the net axial load and net bending moment states with four layers of FRP (M4). Also, the curves of the combined effect of axial load - bending moment of all the M series samples are given in Figure 13.

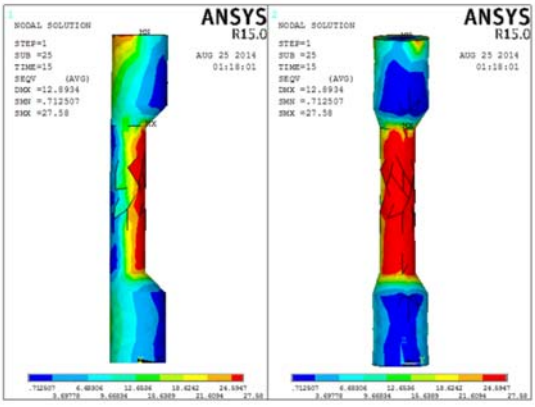

Figure (3): Distribution of stress in the net axial load state (M0)

By distributing stress in the analyzed sample, it was observed that under the net axial load, failure occurs in the middle of the column with a net axial load of 388723N.

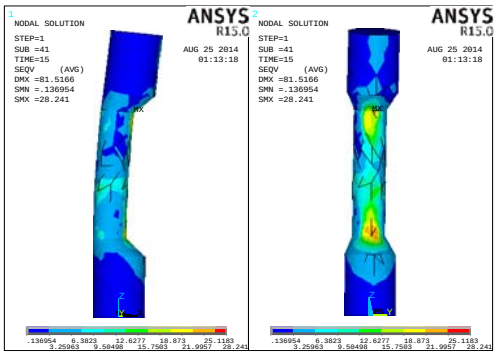

Figure (4): Distribution of stress in the net bending moment state (M0)

When the column is under the flexural column and axial load, section break occurs at the end of the column. The net flexural column is 964200 N.mm.

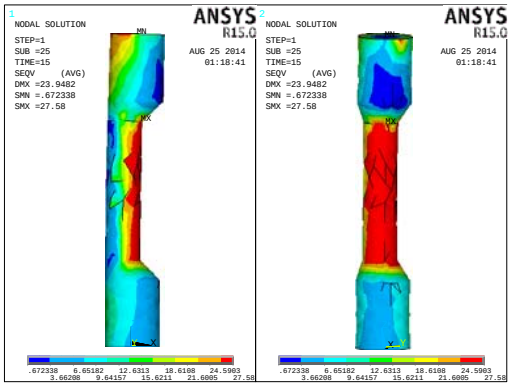

Figure (5): Distribution of stress in the net axial load state (M1)

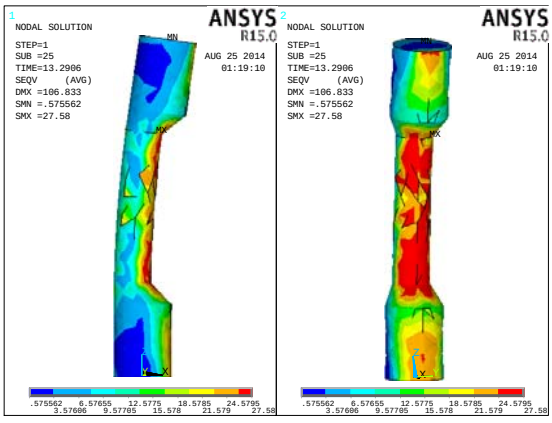

Figures (6): Distribution of stress in the net bending moment state (M1)

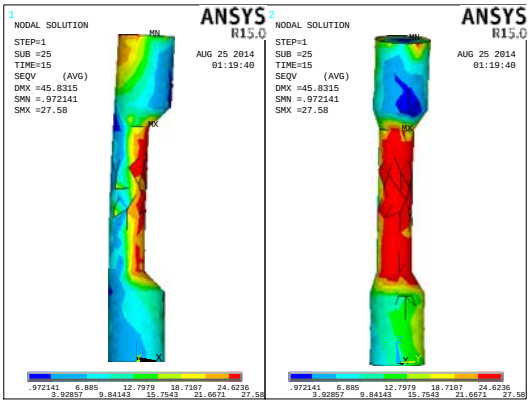

Figures (7): Distribution of stress in the net axial load state (M2)

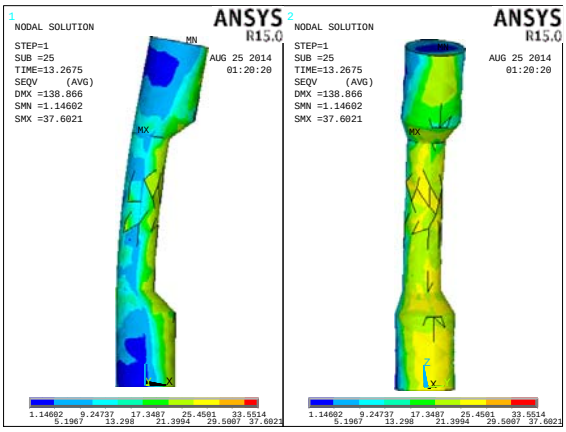

Figures (8): Distribution of stress in the net bending moment state (M2)

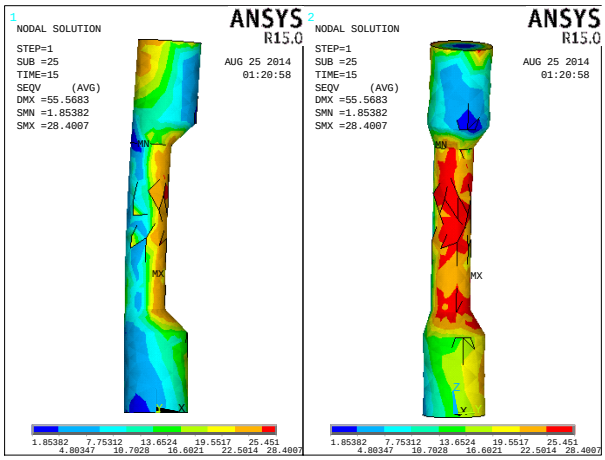

Figures (9): Distribution of stress in the net axial load state (M3)

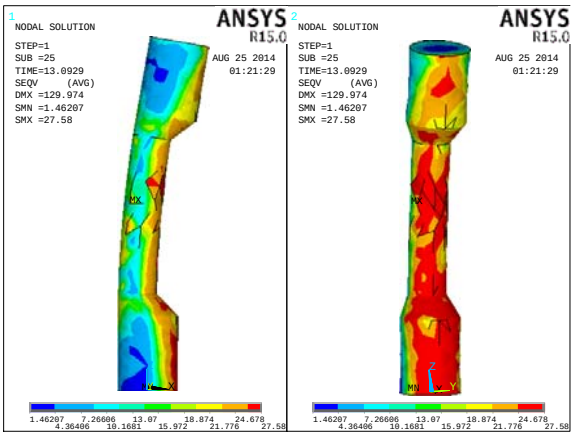

Figures (10): Distribution of stress in the net bending moment state (M3)

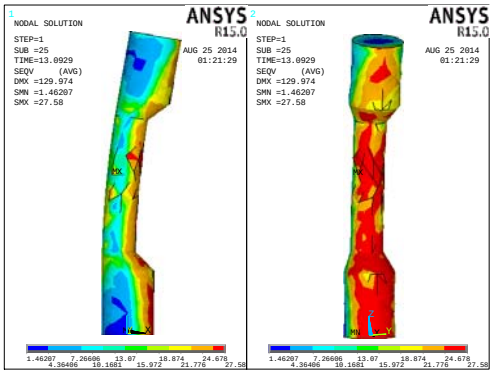

Figures (11): Distribution of stress in the net axial load state (M4)

Given the distribution of stress in the analyzed samples, the column fails when it is under the net axial load, which equals 810921 N.

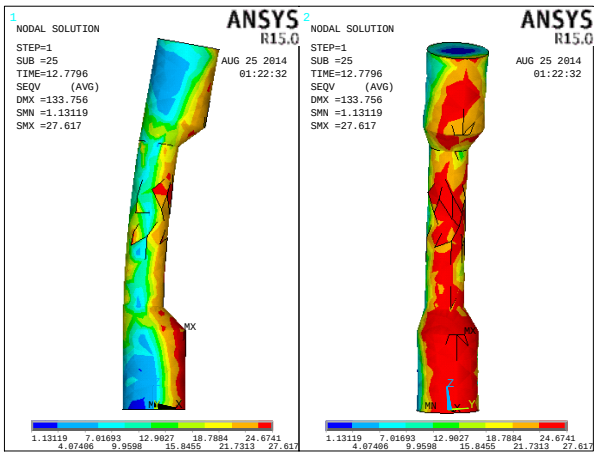

Figure (12): Distribution of stress in the net bending moment state (M4)

The section failure occurs at the end of the column when it is under the bending moment and axial load. The net bending moment is 71470815 N.mm.

M0 is the curve of the combined effect of axial load-bending moment for column without FRP and M1 is the curve of the combined effect of axial load - bending moment for column with one FRP layer. M2 is the curve of the combined effect of axial load - bending moment for column with two layers of FRP and M3 is the curve of the combined effect of axial load - bending moment for column with three layers of FRP. M4 is the curve of the combined effect of axial load - bending moment for column with four layers of FRP. The net axial load of M2 increased more than that of M1 in the curve of the combined effect of axial load - bending moment. The pure axial load of M4 increased more than that of M3 in the curve of the combined effect of axial load - bending moment.

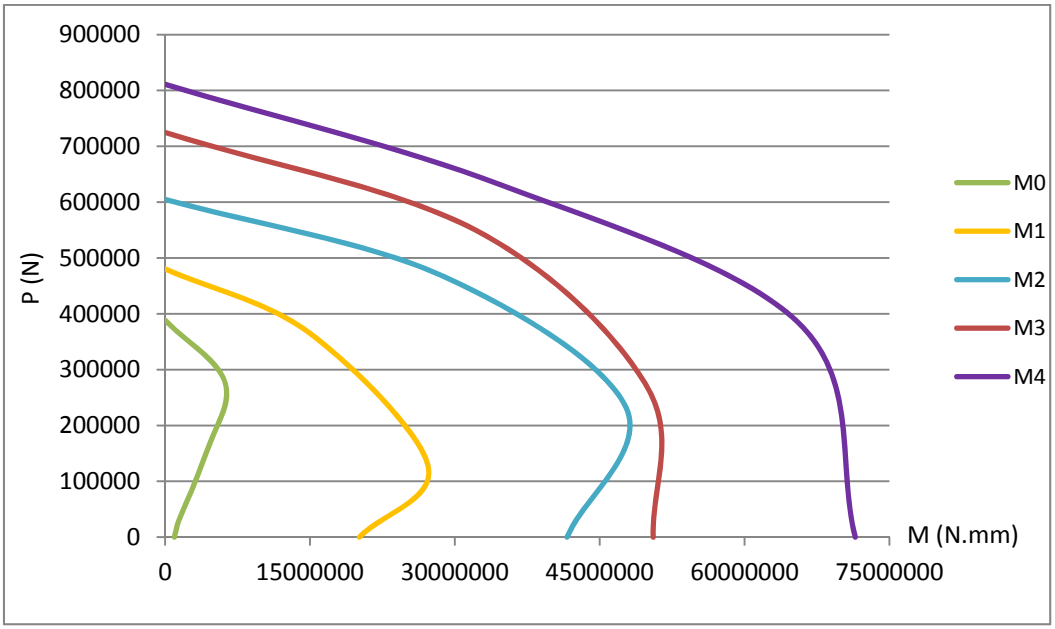

Figure (13): The curves of the combined effect of axial load - bending moment for all M series samples

Results from the N Series Samples

The results derived from the ANSYS Software for the N series samples are presented in Table 2. The size of the column in the N series of Hadi's model is doubled.

Table 2. Distribution of net axial load, balance point of the section and net flexural column in the N series samples

	N0		N1		N2		N3		N4	
	Pn(N)	**Mn(N.mm)**	**Pn(N)**	**Mn(N.mm)**	**Pn(N)**	**Mn(N.mm)**	**Pn(N)**	**Mn(N.mm)**	**Pn(N)**	**Mn(N.mm)**
Net axial load	485000	0	716888	0	864846	0	1020000	0	1175780	0
Balance point of the section	384999	25906583	594942	62046501	642307	79241415	753212	80132407	782017	95156790
Net flexural column	0	12042240	0	46234887	0	75247999	0	87318076	0	108137829

The curves of the combined effect of axial load - bending moment for the entire N series samples are shown in Figure 14.

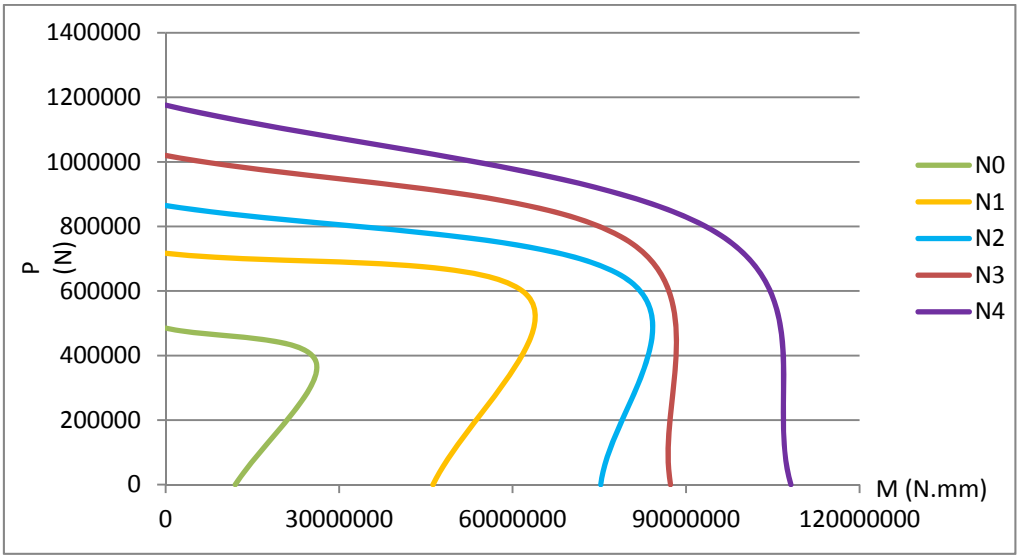

Figure (14): The curves of the combined effect of axial load - bending moment for all N series samples

N0 shows the curve of the combined effect of axial load - bending moment for the column without FRP, N1 is the curve of the combined effect of axial load - bending moment for the column with one layer of FRP, N2 is the curve of the combined effect of axial load - bending moment for the column with two layers of FRP, N3 is the curve of the combined effect of axial load - bending moment for the column with three layers of FRP, and N4 is the curve of the combined effect of axial load - bending moment for the column with four layers of FRP.

By comparing the curves of the combined effect of axial load - bending moment, it was observed that if the number of layers increases from two to three FRP layers, the slope increases in the tension control zone of the section. The same happens when there is an increase from three to four layers of FRP.

CONCLUSIONS

The results of the analysis in this study suggested that:

- Wrapping the column in FRP will increase the load-bearing capacity of the column.
- With an increase in the number of FRP layers, the resistance of the column increases, but this increase is not commensurate with the increase in the number of the layers.
- By comparing the curves of the combined effect of axial load - bending moment, it was observed that if the number of layers increases from 2 to 3 layers of FRP, the slope increases in the tension control zone of the section. The same happens when there is an increase from three to four layers of FRP. It can be concluded that the increase in the number of layers of FRP reduces failure in the tension control zone of the section and this section remains in a state of equilibrium.
- With distribution of stress in all analyzed samples, it was observed that the column fails in the middle when it is under net axial load. The section failure occurs at the end of the column when the column is under axial load and bending moment.
- The results from sampling and modeling by ANSYS 15.0 were complied with the experimental results and thus we inspect the behavior of various samples by the above-mentioned software. Consequently, we will avoid heavy expenses of conducting and repeating the experiments.

REFERENCES

ACI440, American Concrete Institute. (2003). "Guide for the design and construction of concrete reinforced with FRP rebars". ACI 440.1R-03, Farmington Hills, MI, USA.

Balaguru, P., Nanni, A., and Glancapro, J., (2009). "FRP composites for reinforced and prestressed concrete structures".

Canonsburg, P.A. (2009). "ANSYS structural analysis guide: release 12.0". SAS. IP, Inc.

Hadi, M.N.S. (2006). "Behaviour of FRP-wrapped normal-strength concrete columns under eccentric loading". Composite Structures, 72, 503-511.

Hadi, M.N.S. (2007). "The behaviour of FRP wrapped HSC columns under different eccentric loads". Journal of Composite Structures, 78 (4), 560-566.

Karbhari, V.M., and Gao, Y. (1997). "Composite jacketed concrete under uniaxial compression-verification of simple design equations". J. Mater. Civil. Eng., 9 (4), 185-193.

Kusumawardaningish, Y., and Hadi, M.N.S. (2010). "Comparative behaviour of hollow columns confined with FRP composites". Compos. Struct., Doi:10.1016.

Li, J., and Hadi, M.N.S. (2003). "Behaviour of externally confined high-strength concrete columns under eccentric loading". Compos. Struct., 21 (6), 145-153.

Mirmiran, A., Shahawy, M., Samaan, M., and El-Echary, H. (1998). "Effect of column parameters on FRP-confined concrete". Journal of Composites for Construction, 2 (4), 175-185.

Mirmiran, A., Zagers, K., and Yuan, W.Q. (2000). "Non-linear finite element modeling of concrete confined by fiber composites". Finite Elements in Analysis and Design, 35 (1), 79-96.

Mostofinezhad, D., and Saadatmand, H. (2007). "Predicting the behavior of concrete confined in FRP composite with finite element method". International Journal of Iran University of Engineering and Sciences, 18 (2), 55-64.

Mostofinezhad, D., and Saadatmand, H. (2008). "The impact of confinement resulting from CFRP composite on the formatting and resistance of reinforced thin circular concrete columns based on non-linear analysis". Modarres Engineering and Technical Periodical, 33, 33-44.

Parvin, A., and Wang, W. (2001). "Behavior of FRP-jacketed concrete column under eccentric loading". Journal of Composites for Construction, 5 (3), 146-152.

Spoelstra, M.R., and Monti, G. (1999). "FRP-confined concrete model". J. Compos. Constr., 33, 143-150.

Xiao, Y., and Wu, H. (2003). "Compressive behaviour of concrete confined by various types of FRP composite jackets". J. Reinf. Plast. Compos., 22 (13), 1187-1202.